Developmental Biology **226,** 57–72 (2000)
doi:10.1006/dbio.2000.9848, available online at http://www.idealibrary.com on IDEAL®

The *Drosophila Lissencephaly1* (*DLis1*) Gene Is Required for Nuclear Migration

Yiding Lei and Rahul Warrior[1]

Program in Molecular Biology, MC1340, Department of Biological Sciences, University of Southern California, 835 West 37th Street, Los Angeles, California 90089-1340

Nuclear movement is critical for several developmental processes in eukaryotes. *Drosophila* oogenesis provides a paradigmatic example in which localization of the nucleus generates a source of cellular asymmetry that is used in patterning both the anterior–posterior and the dorsal–ventral axes of the oocyte. In this study we show that mutations in the *Drosophila Lissencephaly1* (*DLis1*) gene result in partial ventralization of the eggshell. *DLis1* mutations affect the localization of *gurken* mRNA and protein in the oocyte. These defects are correlated with incorrect positioning of the oocyte nucleus, suggesting that *DLis1* is required for nuclear migration. DLis1 shows significant sequence conservation across the evolutionary spectrum. Fungal cognates of DLis1 are involved in nuclear migration while homologs in humans and mice are implicated in neuronal migration. *DLis1* shows genetic interactions with the Glued and Dynein heavy chain subunits of the dynein/dynactin complex, supporting the idea that the Lis1 family of proteins plays a role in microtubule motor-based nuclear motility. © 2000 Academic Press

Key Words: **Drosophila; nuclear migration; neuronal migration; lissencephaly; dynein; microtubules.**

INTRODUCTION

In a typical eukaryotic cell, the location of the nucleus depends on active processes that move it through the cytoplasm and maintain it at an appropriate subcellular position (reviewed in Reinsch and Gonczy, 1998). Nuclear positioning and migration are also critical in developmental events ranging from fertilization (the migration of male and female pronuclei within the zygote) to organ and tissue differentiation (for example, the characteristic apical to basal nuclear movement seen in the developing vertebrate neural tube; Sauer, 1935; Schatten, 1982). In *Drosophila* there are several developmental processes that are dependent on correct nuclear migration. A striking example is the critical role of oocyte nuclear migration in establishing the polarity of the developing egg. The oocyte nucleus is initially located at the posterior end of the egg. A TGF-α ligand, *gurken* (*grk*), is localized near the nucleus and induces the adjacent follicle cells to follow a posterior rather than the default anterior cell fate (Gonzalez-Reyes *et al.*, 1995; Roth *et al.*, 1995). Midway through oogenesis, the nucleus moves to the anterior margin of the oocyte, where it again signals to the overlying follicle cells (Neuman-Silberberg and Schupbach, 1993). Cells that receive high levels of the *grk* signal acquire dorsal identities, while cells on the opposite side develop as ventral cells. Thus correct migration of the oocyte nucleus is essential for establishment of the anterior–posterior as well as the dorsal–ventral axes of the egg and future embryo (Gonzalez-Reyes *et al.*, 1995; Roth *et al.*, 1995). Nuclear movement is also required for cellularization during *Drosophila* embryogenesis. In early syncytial stages, cleavage nuclei are located in the interior of the embryo. During division cycles 8–10 the nuclei migrate toward the cortex where cellularization is initiated (reviewed in Foe *et al.*, 1993). Failure of these movements results in cellularization defects and embryonic lethality. A third nuclear migration event occurs during morphogenesis and patterning of the eye imaginal disc. It has been shown that cells in the eye disc undergo a stereotypic series of nuclear movements that accompany cell determination (Tomlinson, 1985). Although disruption of nuclear migration in the eye disc does not significantly affect cell specification, it alters cell morphology, resulting in rough eyes (Fischer-Vize and Mosley, 1994).

Studies in fungi have implicated microtubules, as well as the cytoplasmic dynein and dynactin protein complexes in nuclear migration. The microtubule network is thought to

[1] To whom correspondence should be addressed. Fax: (213) 740-0898. E-mail: warrior@mizar.usc.edu.

0012-1606/00 $35.00

provide the basic intracellular framework for motility, while dynein and dynactin contribute motor activity. Cytoplasmic dynein is a large multisubunit complex that can translocate along microtubules toward the minus end. In addition to its role in retrograde axonal transport, dynein has also been implicated in aspects of mitosis and a range of intracellular processes involving minus end-directed transport of membranous organelles and vesicles (reviewed in Holzbaur and Vallee, 1994; Hirokawa, 1998). Dynactin is a second multicomponent complex that is thought to potentiate and regulate dynein activity (Gill *et al.*, 1991). The size and complexity of dynein and dynactin as well as the existence of several cell-type-specific isoforms, suggest that their activities are likely to be regulated at multiple levels (reviewed in Hirokawa, 1998).

Despite the near ubiquitous nature of nuclear migration, relatively little is known about the regulation and cell biology of this process in higher eukaryotes. Studies in *Drosophila* suggest that nuclear migration in higher eukaryotes may also utilize a dynein-based mechanism. The *Drosophila Glued* (*Gl*) gene encodes the p150 component of dynactin, and Gl^{1} mutant flies have rough eyes. In eye imaginal discs from third-instar Gl^{1} larvae, photoreceptor nuclei are randomly distributed, in contrast to the regular apical localization pattern typical of wild-type discs (Harte and Kankel, 1982; Fan and Ready, 1997). This nuclear mislocalization has been attributed to defects in motor activity (Fan and Ready, 1997). Consistent with this hypothesis, heteroallelic combinations of mutations in the *Dynein heavy chain 64C* (*Dhc64C*) gene also have rough eyes (Li *et al.*, 1994).

In addition to known cytoskeletal and motor proteins, phenotypic screens in fungi have identified other genes that are involved in nuclear migration (reviewed in Beckwith *et al.*, 1995). Although the cellular functions of these genes have not been well characterized, they appear to encode molecules that have regulatory rather than structural roles in nuclear migration. Two such genes, *nudC* and *nudF*, were first identified in *Aspergillus* (Osmani *et al.*, 1990; Xiang *et al.*, 1995a). In an earlier study, we isolated the *Drosophila nudC* homolog (*DnudC*) and showed that it was both structurally and functionally conserved (Cunniff *et al.*, 1997). More recently, the functional conservation of *nudC* homologs has been shown to extend across species to human *nudC* (Morris *et al.*, 1997; Miller *et al.*, 1999). In *Aspergillus*, NudC acts by regulating the level of NudF, a critical intermediate in the nuclear migration pathway (Xiang *et al.*, 1995a). A human homolog of *nudF*, called *LIS1*, has been identified and is implicated in the inherited birth defect Miller–Dieker lissencephaly (Reiner *et al.*, 1993). Interestingly, lissencephaly is characterized by defects in neuronal migration in the cerebral cortex, suggesting a mechanistic link between neuronal and nuclear migration.

In order to understand the regulation of nuclear migration in *Drosophila* we have cloned and characterized *Drosophila Lissencephaly1* (*DLis1*), a homolog of the *LIS1* and *nudF* genes. We have isolated mutations in *DLis1* and determined that it is essential for viability. We find that reduction in levels of *DLis1* results in defects in nuclear migration during oogenesis. *DLis1* alleles show genetic interactions with mutations in the *Gl* and *Dhc64C* genes, suggesting that these gene products are functionally linked. These findings indicate that *DLis1* is a component of an evolutionarily conserved pathway mediating nuclear migration.

MATERIALS AND METHODS

Isolation of DLis1 Genomic Clones

Genomic clones for *DLis1* were isolated by screening a bacteriophage Lambda FIX II library generated from Canton-S flies (Stratagene) with probes from the *Aspergillus nudF* and mouse *Lis1* genes. The *Aspergillus* probe was derived from a 1.5-kb *Xho*I–*Nco*I fragment isolated from plasmid pEG202 and included the complete *nudF* coding region (Xiang *et al.*, 1995a). A 0.7-kb fragment containing mouse *Lis1* sequences was obtained by PCR amplification from a mouse liver cDNA template using the oligonucleotide primers mNudF2F (CAGCCAAAATGGTGCTGTCC) and mNudF2R (GCACAGTCTGGTCATTGGAACAG). The mouse and *Aspergillus* probes were used to screen duplicate lifts from the genomic library. Hybridizations were carried out in 5× SSPE, 30% formamide, 1× Denhardt's, 1% SDS at 42°C. Filters were washed in 1× SSPE, 0.5% SDS at 45°C. Both probes hybridized to an identical subset of phage. Restriction and Southern blot analysis of the positive clones identified a 1-kb genomic fragment responsible for the cross-hybridization. This fragment was used to screen a λgt11 cDNA library made from adult Oregon-R flies (Clontech).

Sequencing of DLis1 cDNA and Genomic DNA

Thirty-six *DLis1* cDNA clones were isolated from the phage library and 10 of these were characterized. Both strands of 2 clones with the longest 5′ extension were sequenced using the Sequenase 2.0 kit (United States Biochemical). In addition 6 expressed sequence tag clones were obtained from the *Drosophila* Genome Project. Following restriction analysis, the 5′ and 3′ untranslated regions of 4 of these clones (LD05086, LD14552, LD14405, LD11219) were sequenced.

Molecular Analysis of DLis1 Alleles

The molecular lesions for four representative *DLis1* alleles were characterized. Genomic DNA was prepared from ~20 heterozygous adult flies. The entire *DLis1* coding region was amplified using nested PCR primers (DLisD 5′TGAGAAGTAAGCACAACCC, DLisE 5′CAAGAGTTGAAGGCGGATAAC, and 10T7 5′ACCCTTGCCGATTCTTCC). The PCR fragments were gel purified prior to sequencing using ^{33}P-dideoxy nucleotides (Thermosequenase; Amersham Life Sciences). Three of the mutations resulted from single nucleotide changes. In $DLis1^{3\text{-}1\text{-}2}$, a C → T transition changed CAG (Gln62) to TAG (stop codon); in $DLis1^{1\text{-}2\text{-}2}$, a G → A transition converted a TGG (Trp220) to TGA (stop codon); and in the $DLis1^{8\text{-}25\text{-}3}$ mutation, a conserved Ser (TCC167) was substituted by Phe (TTC), due to a C → T transition. The lesion in $DLis1^{11\text{-}4\text{-}13}$ resulted from a 7-nucleotide insertion GCGGTAG resulting in a reading frame change that converted Tyr (UAC395) to termination (UAG), thus truncating the protein.

Isolation of EMS Alleles for DLis1

A detailed description of the mutagenesis will be presented elsewhere (Liu *et al.*, in preparation). Briefly, isogenic *cn bw* males were mutagenized with 25 mM EMS and crossed with *Elp*/*CyO* virgins. Single F1 males were crossed with *Df(2R)JP6*/*CyO* females. One hundred eighty-three lethal lines were established from a total of approximately 18,000 chromosomes screened. Nine of these lines corresponded to mutations in *DLis1*.

Drosophila Stocks

Mutant stocks utilized were obtained from the *Drosophila* stock centers at Bloomington and Umea. Kin:β-gal localization was monitored using the KL503 insertion line (Clark *et al.*, 1994) and oocyte nuclei were visualized by crossing the P(lacZ, ry^{+})7744, ry^{506} line (obtained from C. A. Berg) into various *DLis1* mutant backgrounds. *Df(3L)10H*, a deficiency for the *Dhc64C* locus, was obtained from T. Hays.

Staining Procedures for Microscopy

Immunocytochemistry, β-galactosidase activity staining, and *in situ* hybridization experiments were carried out using standard protocols (Verheyen and Cooley, 1994). DNA probes used for *in situ* hybridizations were prepared from *bcd*, *osk*, and *grk* plasmids provided by C. Berg (Berleth *et al.*, 1988; Ephrussi *et al.*, 1991; Neuman-Silberberg *et al.*, 1993). The polyclonal rat anti-Grk antibody was obtained from T. Schupbach and used at a 1:3000 dilution (Roth *et al.*, 1995). Dynein heavy chain antibody was used at 1:100 dilution (Santa Cruz Biotechnology). β-Galactosidase expression was visualized using either a mouse monoclonal antibody (Promega) or a rabbit polyclonal antiserum (Cappel).

Newly eclosed female flies were transferred to freshly yeasted vials for 2–4 days prior to dissection. Ovaries were dissected in *Drosophila* Ringers buffer and held on ice until fixation. For visualization of *grk* protein, ovaries were fixed and processed as described in Neuman-Silberberg *et al.* (1996). For other antibodies standard protocols for ovary staining were used (Verheyen *et al.*, 1994). Samples were mounted in Vectorshield anti-fade mountant (Vector Laboratories) before observation under fluorescence or differential interference microscopy with a Nikon Microphot FXA microscope. Dorsal appendage morphology was examined by mounting washed eggs in Hoyers–lactic acid prior to observation using dark-field microscopy. Confocal microscopy was carried out using a Bio-Rad MRC 600 laser scanning confocal microscope. Images were collected using COMOS software and were processed using Adobe PhotoShop 5.0.

Analysis of Gastrulating Embryos

The pattern of gastrulation in wild-type and mutant embryos was monitored in living embryos in Voltalef 3S halocarbon oil. The embryos were observed under transmitted light and photographed at 15-min intervals during the first 3 h of development and at 30-min intervals thereafter.

RESULTS

Molecular Cloning of the DLis1 Gene

The *DLis1* gene was isolated by screening a *Drosophila* genomic library with probes derived from the mouse *Lis1* gene and the *Aspergillus nudF* coding sequence, under conditions of reduced stringency (see Materials and Methods). The hybridizing bacteriophage were plaque purified, restriction mapped, and reprobed to identify genomic fragments responsible for cross-hybridization. The smallest cross-hybridizing fragment was used to screen adult and embryonic cDNA libraries under stringent conditions. After restriction mapping, the two longest cDNA clones were sequenced and found to be identical in the coding region. In addition the cDNA sequences are essentially identical in the region of overlap to partial sequences from 14 expressed sequence tag (EST) clones identified by the Berkeley *Drosophila* Genome Project (BDGP). Based on sequence comparison data, these cDNAs encode *DLis1*, the *Drosophila* homolog of *Lis1*, and *nudF*.

Conceptual translation reveals that *DLis1* encodes a 411-amino-acid protein that shows a high level of sequence identity with its vertebrate homologs (Figs. 1A and 1B). The human and mouse Lis1 proteins differ by a single amino acid and share 69% sequence identity with DLis1. The evolutionary conservation of this family of proteins is underscored by the fact that DLis1 shares 43% identical residues with *Aspergillus* NudF and is 24% identical to Pac1, a protein required for nuclear migration in *Saccharomyces* (Fig. 1B and data not shown; Reiner *et al.*, 1993; Peterfy *et al.*, 1994; Xiang *et al.*, 1995a; Geiser *et al.*, 1997). Like its human and fungal homologs, DLis1 has a predicted α-helical coiled-coil domain in the N-terminal region, followed by seven copies of a GH-WD motif (Figs. 1A and 1B; Xiang *et al.*, 1995a; Lupas, 1996; Geiser *et al.*, 1997). As in the human protein, the fourth and fifth repeats in DLis1 are separated by a large spacer sequence. In the G-protein subunit β-transducin, for which the crystal structure is known, the seven WD repeats fold into a circular propeller-like shape with seven blades. Each blade of the β-propeller consists of four anti-parallel β-sheets and is thought to provide a surface for protein–protein interaction (Sondek *et al.*, 1996; reviewed in Smith *et al.*, 1999). Manual alignment of DLis1 and β-transducin sequences followed by secondary structure prediction using the Insight II molecular modeling program suggests that DLis1 can also form a seven-bladed β-propeller structure (data not shown). Data from biophysical and biochemical characterization of human LIS1 protein are consistent with the idea that it folds into a β-propeller structure *in vivo* (Garcia-Higuera *et al.*, 1996).

Genomic Organization and Transcriptional Analysis of the DLis1 Locus

Analysis of the *DLis1* locus reveals a high level of transcriptional complexity (Fig. 1C). The genomic region that includes *DLis1* has been completely sequenced and 14 EST clones that contain the *DLis1* open reading frame have been partially characterized by the BDGP. Comparison of the sequences from the 5′ end of the cDNA clones with the

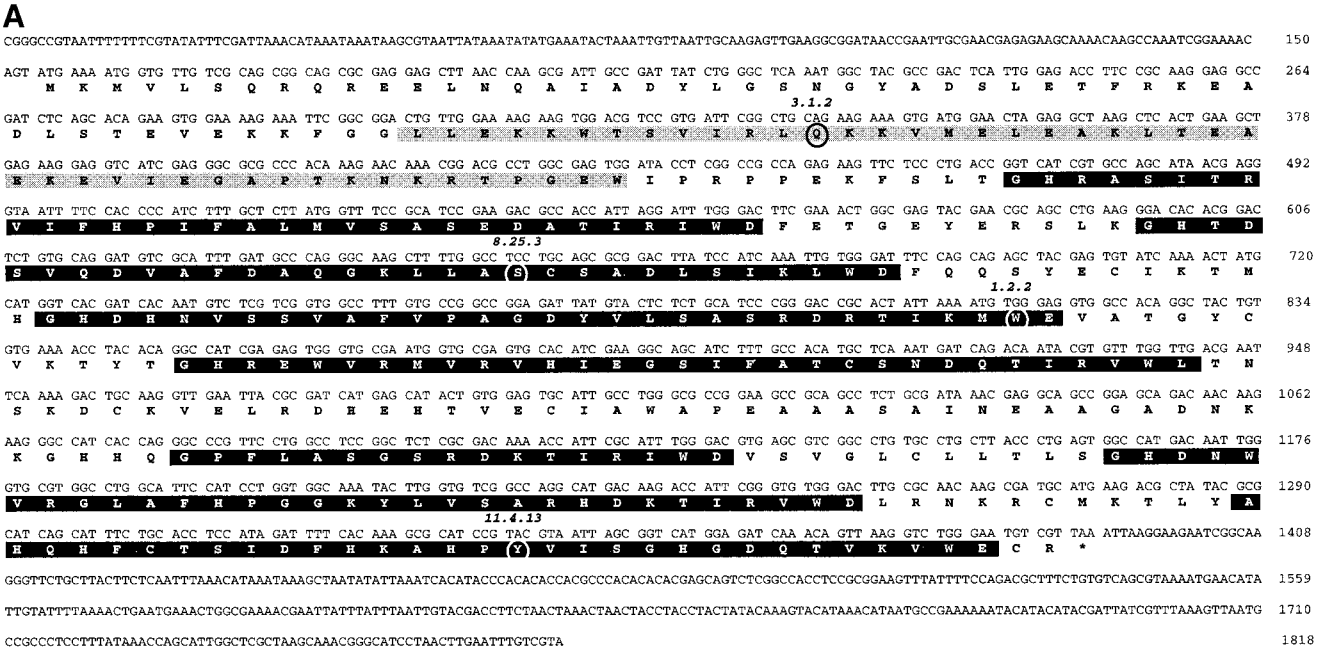

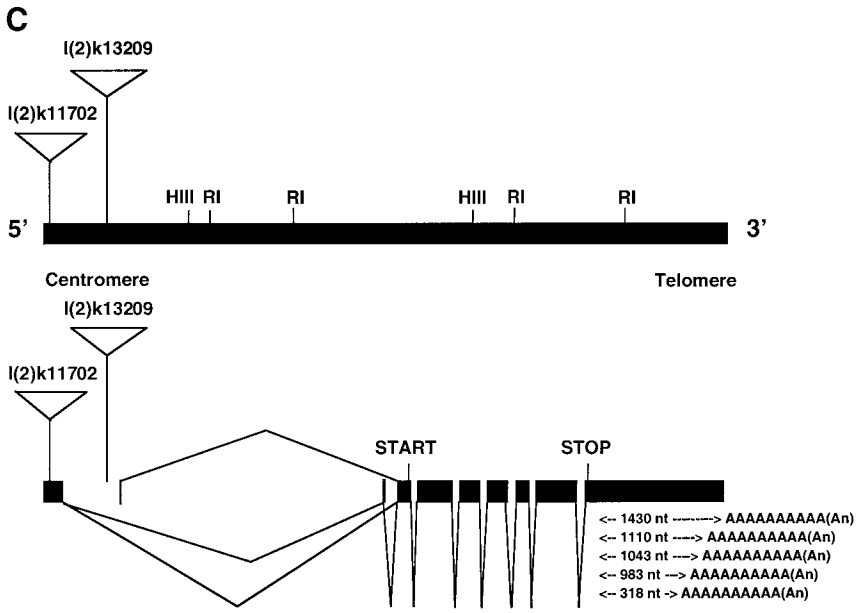

FIG. 1. Primary structure of the *DLis1* gene. (A) Nucleotide and predicted protein sequence of the *DLis1* gene. The nucleotide sequence corresponds to a transcript that originates in the most 5′ exon, is spliced to the common exon that includes the ATG, and terminates at the first polyadenylation site (see C). The amino acid residues encoded by the single ORF are represented in single-letter code. The circles mark residues that are altered in the alleles indicated above. The predicted coiled-coil motif is shaded gray, while the seven GH-WD repeats are highlighted in black. (B) Sequence alignment of the *Drosophila,* human, and *Aspergillus* Lis1 homologs. The DLis1 protein shares 69% identity with human LIS1 and is 43% identical to *Aspergillus* NudF. The sequence identity between the human and the *Drosophila* proteins extends through their entire length. NudF contains 21 residues in the seventh WD repeat that are not present in DLis1 and LIS1. (C) Genomic organization of the *DLis1* locus. The filled bar represents the 6.3-kb genomic region that includes the *DLis1* transcription unit. The two different 5′ exons that are incorporated into three alternately spliced transcripts are indicated. For the five cDNA clones characterized, the length of the 3′ trailer sequence (i.e., the number of nucleotides between the termination codon and the polyadenylation sites) is indicated. The triangles mark the locations of the P-element insertions in $DLis1^{11702}$ and $DLis1^{13209}$.

genomic DNA demonstrates the existence of three alternatively spliced *DLis1* transcripts. Two of the splice variants originate in a common 122-nucleotide 5′ noncoding exon and are spliced either directly or by way of an optional 27-nucleotide exon to the 109-nucleotide exon which contains the translational start site. The initiation site for the third transcript lies 500 nucleotides 3′ of the other two splice variants in a 42-nucleotide noncoding exon and is spliced directly to the exon containing the translation start signal. The six exons that encode the protein are common to all three mRNA isoforms (Fig. 1C). Six of the EST clones were obtained from the genome project and after preliminary analysis by restriction mapping, 4 representative cDNA clones were selected for sequencing. Analysis of these clones showed that they differ in the length of the 3′ untranslated trailer sequence due to the utilization of alternative polyadenylation sites (Fig. 1C). In this context it may be significant that the mouse *Lis1* locus also undergoes alternative splicing of upstream noncoding exons, and *Lis1* genes in humans and mice use at least four alternative polyadenylation sites (Lo Nigro *et al.*, 1997; Peterfy *et al.*, 1998).

Expression Pattern of the DLis1 Gene

Utilization of the alternative polyadenylation sites is predicted to yield transcripts of 1.8, 2.5, 2.55, 2.6, and 2.9 kb. These sizes correspond well to the three broad bands detected at 1.8, 2.5, and 2.9 kb when a developmental Northern blot is hybridized with a *DLis1* probe (Fig. 2A). The small size differences between the differentially spliced variants are below the resolution of agarose gel electrophoresis and they cannot be distinguished on the Northern blot. An additional band seen at 1.6 kb does not correspond to any cDNA or EST clone characterized thus far. *DLis1* mRNA can be found throughout development, although transcript levels are highest in adult females and in early stage embryos.

The spatial distribution of the *DLis1* transcript was determined by *in situ* hybridization with digoxigenin-labeled probes derived from the coding region of the gene (Figs. 2B–2H). During oogenesis *DLis1* is expressed primarily in germ-line cells. Low levels of *DLis1* mRNA can be detected in the germarium in regions 1 and 2 and in both nurse cells and the oocyte in stage 2–4 egg chambers. *DLis1*

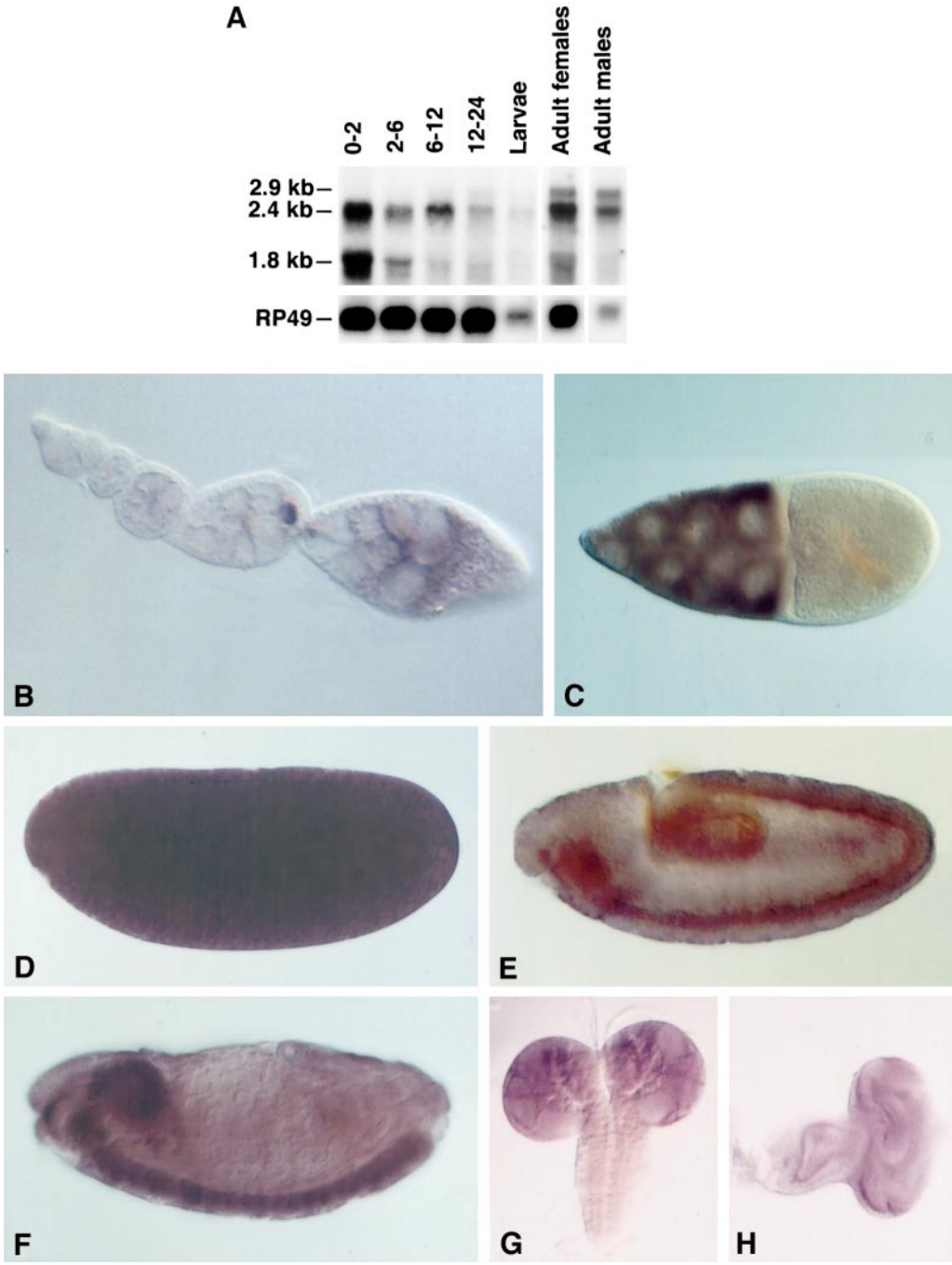

FIG. 2. *DLis1* transcript distribution. (A) Northern blot of poly(A)$^+$ RNA from embryonic, larval, and adult stages hybridized with a probe from the *DLis1* ORF. *DLis1* RNA can be detected throughout development. Three bands of ~1.8, 2.4, and 2.9 kb can be identified. The longest transcript can first be detected in 6- to 12-h embryos and is enriched in adult males. The bottom shows the RP49 loading control. (B) Low levels of *DLis1* transcript are present in germaria and stage 2–4 egg chambers, while higher levels of signal are seen in the oocyte during stages 5–7. (C) *DLis1* mRNA is abundant in the nurse cells during stages 8–10. (D) Syncytial stage embryos contain large amounts of *DLis1* mRNA. (E) By comparison, transcript levels are reduced during gastrulation, but (F) *DLis1* signal accumulates in the central nervous system during later stages of embryogenesis. (G) In third-instar larvae, *DLis1* message is seen in the brain hemispheres and (H) is uniformly distributed in the eye imaginal discs.

message is enriched in the oocyte during stages 5–7; however, in stage 8–10 egg chambers *DLis1* mRNA accumulates at much higher levels in nurse cells (Figs. 2B and 2C). In embryos *DLis1* transcript is most abundant at precellular blastoderm stages, suggesting the presence of a maternal contribution (Fig. 2D). *DLis1* mRNA is ubiquitously distributed in early embryos; however, the levels decline after the onset of gastrulation. Following germ-band retraction it is enriched in the developing central nervous system (Figs. 2E and 2F). In third-instar larvae, low levels of *DLis1* transcript can be detected in the brain hemispheres and imaginal discs (Figs. 2G and 2H).

Isolation of Mutations in DLis1

In situ hybridization to polytene chromosomes revealed that *DLis1* maps to bands 52F–53A and is deleted in *Df(2R)JP6* (data not shown; Saxton *et al.*, 1991). We employed two approaches to recover mutations in *DLis1*. DNA flanking several P-element lethal lines that mapped in the vicinity of the *DLis1* locus was isolated by plasmid rescue and the insertion sites were located on the genomic map. Our analysis revealed that the P element in *l(2)k13209* was inserted in the first intron of *DLis1* (see Fig. 1C). Excision of the P element restored viability, demonstrating that the lethality resulted from the presence of the transposon (data not shown). A second lethal line, *l(2)k11702,* contained a P-element insert in the first exon of *DLis1,* 43 nucleotides downstream of the transcription start site (see Fig. 1C). Henceforth these P-element lines are referred to as $DLis1^{13209}$ and $DLis1^{11702}$. Complementation analysis suggested that the lethality of the $DLis1^{11702}$ stock was not associated with the P insert in *DLis1* (data not shown). We separated the linked lethal mutation from the P-element insertion by recombination and found that homozygous $DLis1^{11702}$ flies are viable but sterile.

In a parallel approach, an EMS mutagenesis screen was carried out to isolate mutations that were lethal *in trans* to *Df(2R)JP6.* A total of 18,000 mutagenized chromosomes were screened and 183 lethal lines established. Sixty-six of these lines mapped within a smaller deficiency, *Df(2R)JP8,* and *inter se* complementation analysis allowed their assignment to 14 different complementation groups (Liu *et al.*, in preparation). Nine independent lines belonging to one group were lethal *in trans* to $DLis1^{13209}$, suggesting that they represent mutations in *DLis1*. In order to confirm this, the genomic region containing the *DLis1* open reading frame from 4 representative *DLis1* mutant lines was amplified using PCR. Direct sequencing revealed that 3 of these alleles ($DLis^{3.1.2}$, $DLis^{1.2.2}$, and $DLis^{11.4.3}$) encode truncated proteins resulting from premature termination codons (see Fig. 1A; Materials and Methods). In the fourth allele, $DLis^{8.25.3}$, a single base pair change results in a phenylalanine to serine substitution at a conserved position (F167S, see Fig. 1A).

Mutations in DLis1 Affect Patterning of the Eggshell

Animals homozygous for all EMS-induced *DLis1* alleles isolated in our screen, as well as the P-element mutant $DLis1^{13209}$, are late larval or early pupal lethals (data not shown). However, flies bearing these alleles *in trans* to the weak $DLis1^{11702}$ allele are viable, but male and female sterile. Eggs laid by such transheterozygous females showed defects in the location and morphology of the dorsal appendages (Figs. 3A–3F). Dorsal appendages are paired paddle-shaped structures that arise from the dorsal-anterior side of the eggshell and are used by the embryo for respiration. Defects in dorsal–ventral as well as anterior–posterior patterning during oogenesis are often associated with alterations in the morphology or placement of the dorsal appendages (reviewed in Nilson and Schupbach, 1999).

We examined eggs laid by females carrying a copy of $DLis1^{11702}$ *in trans* to three different EMS alleles (Table 1b). Based on the severity of the dorsal appendage phenotype the mutant eggs were placed in five categories. Class 1 comprised eggs with apparently normal dorsal appendages, in both their structure and their position (Fig. 3A). In Class 2 eggs the appendages were located closer than normal but remained separate (Fig. 3B). A third class consisted of eggs in which the dorsal appendages were partially fused (Fig. 3C). In Class 4 eggs the dorsal appendages were fused along their entire length to form a single structure (Fig. 3D). In a small fraction of the eggs laid by *DLis1* mutant mothers, the fused dorsal appendages were severely reduced in size and displaced posteriorly (Figs. 3E and 3F). These eggs constitute Class 5. All three *DLis1* alleles tested *in trans* to $DLis1^{11702}$ showed similar defects, although the severity of the phenotype varied in an allele-specific manner (Table 1a). In all cases, greater than 68% of the eggs showed fused dorsal appendages typical of Classes 4 and 5. By comparison, females carrying the EMS alleles or $DLis1^{11702}$ *in trans* to wildtype laid morphologically normal eggs (Table 1). To rule out the possibility that an independent mutation in the background of the EMS alleles is responsible for the defects observed *in trans* to $DLis1^{11702}$, we examined eggs laid by females of the genotype $DLis1^{13209}/DLis1^{11702}$. These eggs also showed dorsal appendage defects at a high frequency (Table 1).

In normal development, the follicle cells provide spatial cues that are required to establish the dorsal–ventral axis of the embryo. Thus many mutations that alter eggshell polarity also perturb patterning of the embryo (Schupbach and Wieschaus, 1991). In order to determine whether reduction in *DLis1* activity resulted in ventralization of the embryos, we crossed $DLis^{3.1.2}/DLis^{11702}$ transheterozygous females to wild-type males and monitored the development of the eggs under halocarbon oil (Fig. 4). Fewer than 20% of the eggs laid undergo cellularization and gastrulation. Of these, about half (10% of the total) show obvious signs of ventralization. During early gastrulation the cephalic furrow that normally occupies a lateral position is displaced

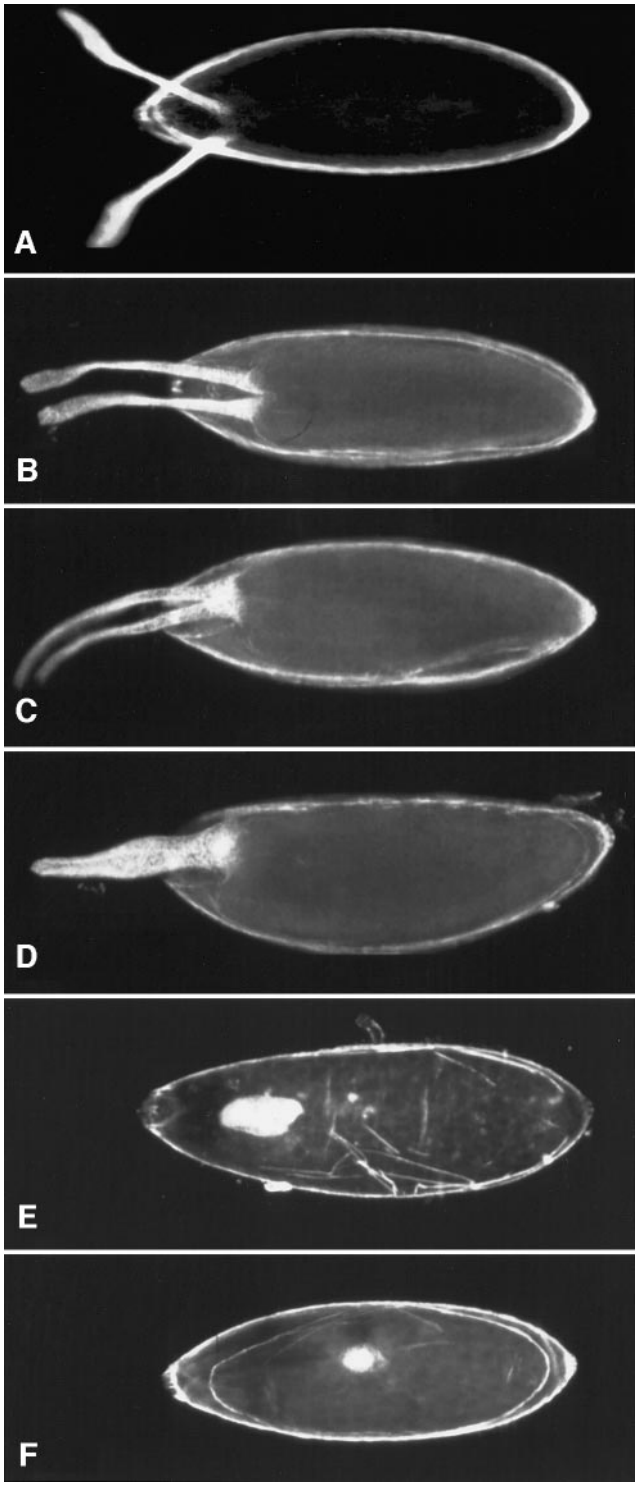

FIG. 3. Loss of *DLis1* activity results in ventralization of the eggshell. Dark-field view of eggs laid by *DLis1* mutant females (genotypes listed in Table 1). Anterior is to the left, and dorsal side is facing the viewer. (A) A wild-type Class I egg with two paddle-like dorsal appendages that are separate from each other and located at the anterior. (B) Class II eggs are characterized by appendages that are distinct but abnormally close to each other (C) Class III eggs bear dorsal appendages that are partially fused at the base, while in Class IV eggs (D) the dorsal appendages are fused along their entire length to form a single structure. (E and F) Eggs in which the dorsal appendages are reduced and displaced posteriorly, (Class V).

dorsally (marked with an arrowhead in Figs. 4A and 4E), indicating that the dorsal cells have acquired a more ventral identity. *DLis1* mutants also show defects in germ-band extension consistent with a shift in cell fate along the dorsal–ventral axis. Germ-band extension is delayed in mutant embryos with respect to wildtype (compare Figs. 4A and 4E) and does not extend as far anteriorly (Figs. 4C and 4G). At later stages, the germ-band fails to extend completely and instead invaginates into the interior of the embryo (see arrows in Figs. 4D and 4H). However, the majority of these embryos fail to complete embryogenesis. This was confirmed by examining cuticle preparations of egg lays from *DLis1* mutant mothers. Only a small fraction of the embryos (<5%) differentiate a cuticle, all of which were wild-type in appearance.

DLis1 Interacts Genetically with grk and torpedo

The defects observed in *DLis1* transheterozygotes are similar to those caused by reduction in EGF signaling (reviewed in Nilson and Schupbach, 1999). We therefore tested for genetic interactions between *DLis1* and components of the EGF signaling pathway, such as *grk*, *torpedo* (*top*), and *cornichon* (*cni*). We observed a strong enhancement of the eggshell phenotype in flies double heterozygous for $DLis1^{11702}$ and the strong grk^{HK36} allele. About 68% of the eggs laid by such females showed completely fused dorsal appendages typical of Classes 4 and 5 (see Table 1). Similar phenotypes were observed with other *DLis1* alleles *in trans* to grk^{HK36} (Table 1; data not shown). Flies double heterozygous for *DLis1* and top^{CO}, a strong loss-of-function mutation in the EGF receptor, also displayed a significant increase in the frequency of fused dorsal appendages in comparison to the control females. In contrast, only weak interactions were detected between *DLis1* and the cni^{AR} and cni^{AA} alleles (Table 1; data not shown).

grk mRNA and Protein Are Aberrantly Localized in DLis1 Mutants

The ventralized chorion phenotype resulting from reduction in *DLis1* activity, as well as the genetic interactions observed between *DLis1* and components of the EGF signaling pathway, raised the possibility that *DLis1* is required for localization of the *grk* ligand. In order to test this, the distribution of *grk* mRNA was examined in ovaries from females transheterozygous for $DLis1^{11702}$ and different *DLis1* alleles. In wild-type egg chambers from stages 1–7

TABLE 1
Dorsal Appendage Defects in *DLis1* Mutant Eggs

Genotype of female	Dorsal appendage phenotype				
	Class I	Class II	Class III	Class IV	Class V
a. controls					
$DLis1^{11702}/+$	99%	1%	—	—	—
$DLis1^{13209}/+$	98%	2%	—	—	—
$DLis1^{3.1.2}/+$	96%	4%	—	—	—
$DLis1^{8.25.3}/+$	100%	—	—	—	—
$DLis1^{11.4.13}/+$	99%	1%	—	—	—
$Df(2R)JP8/+$	95%	5%	—	—	—
$grk^{HK36}/+$	49%	45%	3%	3%	—
$top^{CO}/+$	98%	2%	—	—	—
$cni^{AA}/+$	100%	—	—	—	—
b. Double heterozygotes					
$DLis1^{11702}/DLis1^{3.1.2}$	3%	15%	6%	70%	6%
$DLis1^{11702}/DLis1^{8.25.3}$	12%	4%	15%	62%	7%
$DLis1^{11702}/DLis1^{11.4.13}$	2%	12%	15%	68%	3%
$DLis1^{11702}/DLis1^{13209}$	21%	19%	14%	45%	1%
$DLis1^{11702}/Df(2R)JP8$	40%	10%	26%	24%	—
$DLis1^{11702}/grk^{HK36}$	1%	5%	26%	68%	—
$DLis1^{3.1.2}/grk^{HK36}$	0%	2%	6%	92%	—
$DLis1^{11702}/top^{CO}$	6%	55%	32%	7%	—
$cni^{AA}/DLis1^{11702}$	98%	2%	—	—	—

Note. Eggs laid by females of the genotypes listed were classified based on the severity of the dorsal appendage phenotype. Class 1, apparently wildtype; Class 2, closer than wildtype; Class 3, fused at the base; Class 4, fused along their entire length. Class 5 includes eggs with the most severe phenotype in which the dorsal appendages were highly reduced in size and displaced posteriorly. A minimum of 200 eggs from independent egg lays were scored for each genotype.

grk transcript is localized in a crescent between the oocyte nucleus and the posterior of the oocyte. At stage 8, the microtubule cytoskeleton undergoes a reorientation and the oocyte nucleus migrates to the anterior. Consequently *grk* mRNA accumulates transiently along the anterior margin of the oocyte and from late stage 8 onward is tightly localized around the dorsal anterior side of the oocyte nucleus (Fig. 5A; Neuman-Silberberg *et al.*, 1993; Roth *et al.*, 1995). In *DLis1* mutant ovaries, no abnormalities were observed in *grk* mRNA localization during stages 1–7. However, from stage 8 onward *grk* message was mislocalized in 10–20% of mutant egg chambers, depending on the strength of the allelic combination. Most frequently, the transcript was less tightly confined to the anterior cortex compared to wildtype. In about 5% of the egg chambers, *grk* mRNA was detected in the middle of the oocyte rather than at the anterior, in association with an abnormally positioned oocyte nucleus (Fig. 5B). Ovaries from *DLis1* transheterozygotes were also stained with polyclonal antisera against *grk* protein to determine the extent to which localization of the ligand was perturbed. Consistent with the effects on *grk* transcript, *grk* protein distribution was essentially normal in early egg chambers. However, from stage 8 onward, *grk* protein appeared to be less tightly localized or mislocalized in *DLis1* mutant egg chambers. In addition the level of staining was lower than in comparably staged wild-type oocytes (Figs. 5C and 5D).

The preceding results indicated that the altered distribution of *grk* mRNA could be a consequence of the mislocalization of the oocyte nucleus. Therefore we directly examined the position of the germinal vesicle in *DLis1* mutant egg chambers. A P-element enhancer trap line that drives *β*-galactosidase expression in the nuclei of germ-line cells was crossed into a *DLis1* mutant background. Ovaries from $DLis1^{11702}/DLis1^{3.1.2}$ flies were dissected and lacZ expression in the oocyte nucleus was visualized by activity staining. In ~8% of stage 9–10 egg chambers, the nucleus was misplaced and located approximately midway along the anterior–posterior axis of the oocyte (Figs. 5E and 5F). The frequency of nuclear mislocalization correlated well with the most severe fused dorsal appendage phenotype and the instances of mislocalization of *grk* mRNA to the center of the oocyte (see Table1 and Fig. 5B). An additional 13% of the egg chambers showed less severe but detectable displacement of the oocyte nucleus. Similar effects were observed in eggs from females of the genotype $DLis1^{11702}/DLis1^{8.25.3}$ and $DLis1^{11702}/DLis1^{11.4.13}$ (data not shown).

The mislocalization of *grk* mRNA in *DLis1* transheterozygotes could result from defects in the machinery involved in general transcript localization during oogenesis.

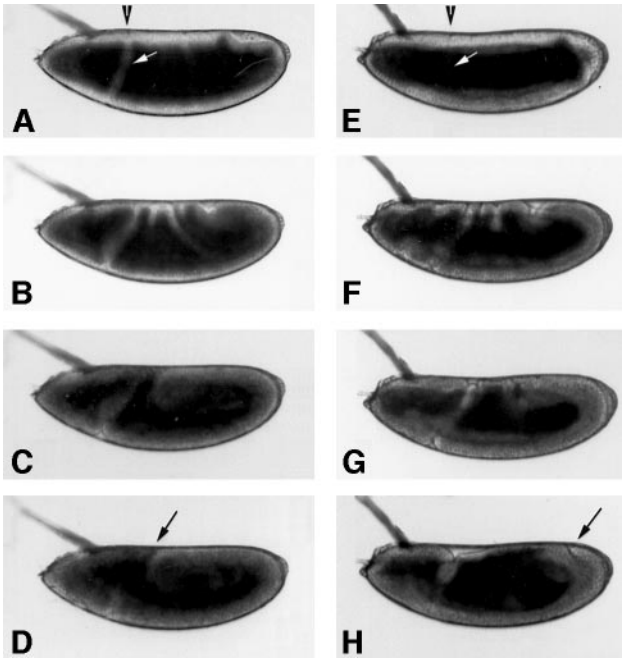

FIG. 4. *DLis1* mutant embryos show fate map changes along the dorsal–ventral axis. Time-lapse photographs of gastrulation movements in wild-type (A–D) and *DLis1* mutant embryos (E–H). The normally lateral cephalic fold in wild-type embryos (A, open arrowhead) is shifted to the dorsal side in *DLis1* mutants (E). The arrow in (A) marks the cephalic furrow at its normal location, while in (E) the arrow points to the absence of a furrow at this location in the mutant. Germ-band extension also proceeds abnormally in *DLis1* embryos (compare B–D with F–H). In mutant embryos the germ band does not extend anteriorly along the dorsal surface, and instead it invaginates into the interior (compare C, D with G, H). Arrows mark the anterior limit of the germ band on the dorsal surface. *DLis1* mutant embryos display the prominent cephalic fold characteristic of ventralized embryos (H).

In this event one might expect that other localized mRNAs would be aberrantly distributed in *DLis1* ovaries. To test this idea we examined the distribution of *bicoid* (*bcd*) and *oskar* (*osk*), two well-characterized transcripts that are normally localized to opposite ends of the mature oocyte. In wild-type stage 8–10 egg chambers *bcd* mRNA is confined to the anterior margin of the oocyte, while *osk* mRNA is present at the posterior pole of the oocyte (Berleth *et al.*, 1988; Ephrussi *et al.*, 1991; Kim Ha *et al.*, 1991). We did not detect any difference in the abundance or localization of either *osk* or *bcd* transcripts in ovaries from *DLis1* transheterozygotes (Figs. 5G and 5H; data not shown).

In order to determine whether loss of *DLis1* activity affects some global aspect of the microtubule cytoskeleton we examined the distribution of a protein containing the motor domain of the plus-end-directed microtubule motor kinesin fused to β-galactosidase (Kin:βgal; Giniger *et al.*, 1993; Clark *et al.*, 1994). Kin:βgal protein accumulates at the plus ends of microtubules in the oocyte as well as in neurons and columnar epithelial cells, and its localization has been used as a sensitive assay for the polarity and integrity of the microtubule network (Gonzalez-Reyes *et al.*, 1995; McGrail *et al.*, 1995; Roth *et al.*, 1995; Clegg *et al.*, 1997). In wild-type egg chambers Kin:βgal is transiently localized to the posterior of the oocyte during stages 8–9. This localization is lost at stage 10, with the initiation of cytoplasmic streaming in the oocyte (Clark *et al.*, 1994). We examined stage 9 egg chambers from $DLis1^{11702}/DLis1^{3.1.2}$ females and found that Kin:βgal was tightly focused to the posterior in a majority of the egg chambers (92%; Fig. 6A). In the remaining cases the fusion protein was present at the posterior of the oocyte but less tightly localized (data not shown). In comparison, Kin:βgal was found at the posterior in 100% of wild-type stage 9 egg chambers examined, suggesting that the microtubule cytoskeleton and kinesin activity are largely unaffected in $DLis1^{11702}/DLis1^{3.1.2}$ egg chambers.

The minus-end-directed motor cytoplasmic dynein has been implicated in nuclear migration in several fungal systems. In addition, genetic epistasis data suggest that *nudF*, the *Aspergillus* homolog of *DLis1*, acts upstream of dynein in mediating nuclear migration (Xiang *et al.*, 1995a). We therefore examined *DLis1* egg chambers to determine whether the level or distribution of *Dhc64C* protein was affected. In wild-type ovaries high levels of Dhc64C can be detected in the oocyte from region 2 in the germarium onward (Li *et al.*, 1994). Later, in stage 9 egg chambers Dhc64C is enriched at the posterior of the oocyte and also outlines the oocyte nucleus (Fig. 6B; Li *et al.*, 1994). In *DLis1* mutants Dhc64C localization appeared unperturbed through early oogenesis. However, in stage 9 mutant egg chambers localization to the posterior of the oocyte was strongly reduced, suggesting that *DLis1* activity is required for dynein localization or activity (Fig. 6C).

DLis1 Shows Genetic Interactions with the Cytoskeletal Motor Components Glued and Dynein heavy chain 64C

The dependence of dynein localization on DLis1 activity suggested a functional interaction between these two genes. We therefore tested whether the *DLis1* phenotype was affected by mutations in the *Gl* and *Dhc64C* genes that encode structural components of the dynein–dynactin microtubule motor (Swaroop *et al.*, 1987; Gill *et al.*, 1991; Holzbaur *et al.*, 1991; Hays *et al.*, 1994). We found that the Gl^1 allele caused a synthetic lethality with strong heteroallelic combinations of *DLis1* mutations, while in combinations with weaker *DLis1* alleles Gl^1 caused a reduction in viability (Table 2). Adult escapers from the latter crosses generally did not survive for more than a few days. More interestingly, they displayed defects in eye morphology, bristles, and abdominal tergites (Fig. 7; data not shown). Flies carrying the dominant Gl^1 allele have small, rough eyes with irregularly positioned bristles (Figs. 7A and 7B;

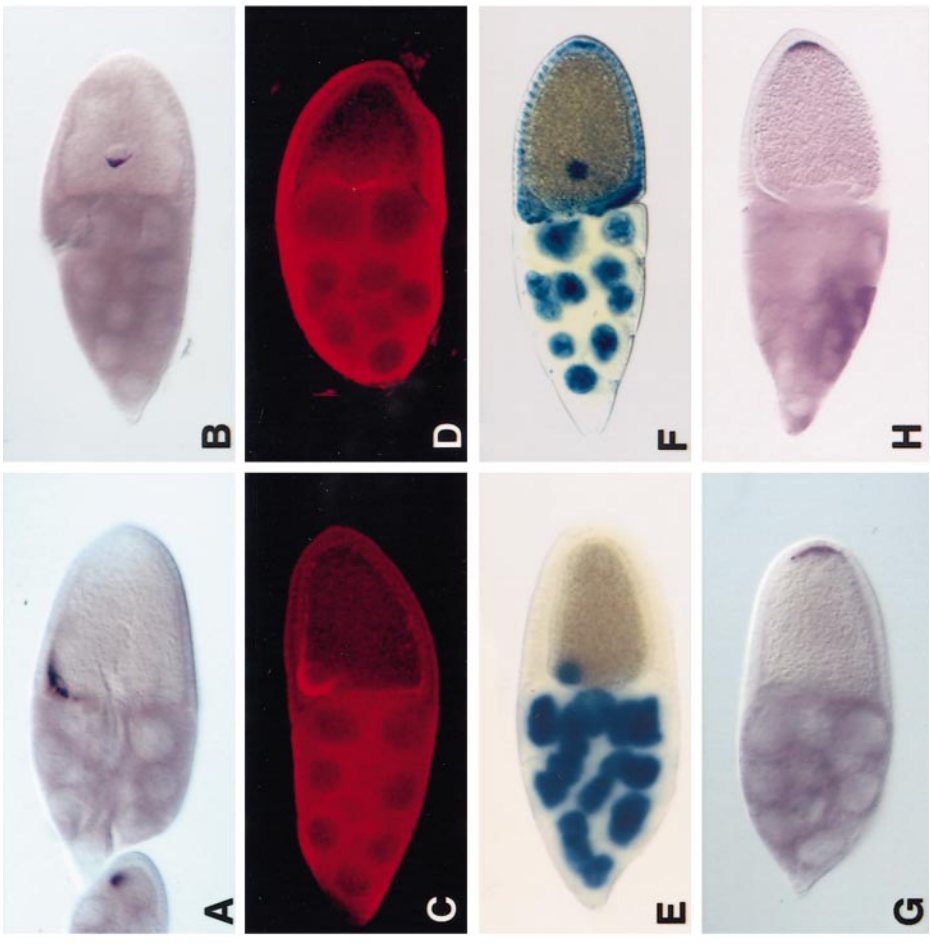

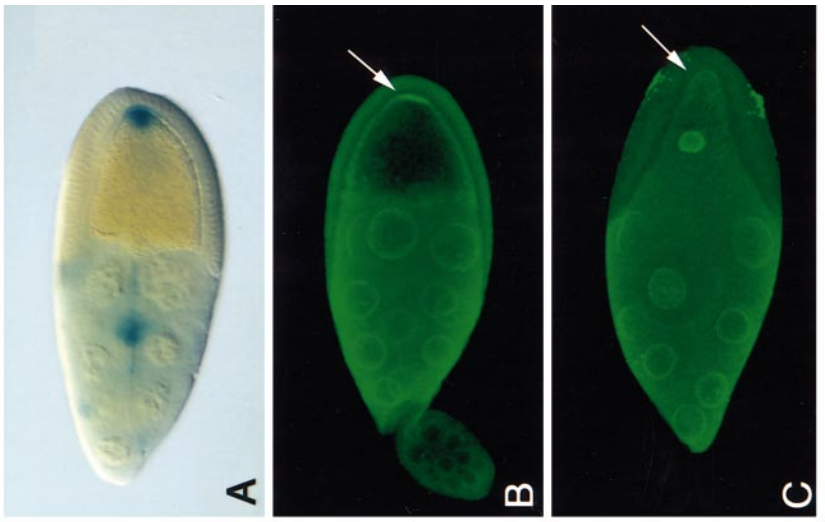

FIG. 5. Reduction in *DLis1* activity affects positioning of the oocyte nucleus and *grk* localization. (A) In wild-type egg chambers *grk* mRNA and the oocyte nucleus are tightly localized at the future dorsal anterior region of the egg. (B) In strongly affected *DLis1* egg chambers *grk* transcript is mislocalized to the middle of the oocyte along with the nucleus. Antibody stains show that in wild-type eggs (C) *grk* protein is confined to the anterior cortex surrounding the nucleus, while in *DLis1* females (D) Grk is mislocalized and levels are reduced. (E) In wild-type egg chambers, the oocyte nucleus (marked by expression of a nuclear *β*gal enhancer trap) is located at the anterior margin of the oocyte, but in mutant egg chambers (F) the nucleus is displaced posteriorly. Despite the defects in *grk* localization, *osk* mRNA is normally localized to the posterior of the oocyte in eggs from *DLis1* females (H, compare with wildtype, G).

FIG. 6. Kin:*β*gal localization appears unaffected in *DLis1* mutants. (A) Kin:*β*gal fusion protein is localized normally to the posterior of the oocyte in egg chambers with reduced levels of *DLis1*. In contrast, reduced levels of dynein heavy chain are present at the posterior of stage 9 *DLis1* (C) compared to wild-type (B) egg chambers.

TABLE 2

Survival of *DLis1* Transheterozygous Adults in Combination with Gl^1

Genotype of male parent	Genotype of progeny	
	$DLis1^x/DLis1^{11702}$; +/+	$DLis1^x/DLis1^{11702}$; Gl^1/+
$DLis1^{7.13.1}$	81%	0%
$DLis1^{8.25.3}$	89%	1.5%
$DLis1^{11.4.13}$	110%	8.3%
$DLis1^{3.1.2}$	85%	15.8%
$DLis1^{3.3.1}$	87%	50%

Note. Male flies indicated in column 1 were mated with females of the genotype $DLis1^{11702}/CyO$; +/+ (data reported in column 2) or $DLis1^{11702}/CyO$; $Gl^1/TM3Sb$ (data reported in column 3). A minimum of 200 progeny were scored for each cross. Progeny of the genotypes indicated in columns 2 and 3 are reported as % observed/expected.

Harte *et al.*, 1982; Fan *et al.*, 1997). A reduction in *DLis1* activity resulted in an enhancement of the Gl^1 eye phenotype (Figs. 7A–7C). In addition the scutellar bristles of escaper flies were reduced in size and frequently lost (Figs. 7D and 7E). Most adult escapers lacked bristles on the ventral side of the abdomen, and in many animals abdominal tergites were completely absent in one or more segments (data not shown). *DLis1* mutants showed similar but weaker interactions with *Dhc64C* alleles. A deficiency for *Dhc64C* (*Df(3L)10H*) was viable in combination with *DLis1* mutants. However, the adults displayed defects in scutellar and abdominal bristle morphology resembling those seen in $DLis1^{8.25.3}/DLis1^{11702}$; Gl^1/+ adults (data not shown). Thus the genetic interactions between *Dhc64C*, *Gl* and *DLis1* are consistent with a functional relationship between these genes.

DISCUSSION

In this study we have characterized the *DLis1* gene and presented evidence for the existence of a conserved pathway involved in nuclear migration in higher eukaryotes. Our results suggest that the defects seen in *DLis1* mutants are linked to dynein-mediated microtubule-based motility.

Functional Analysis of DLis1

The *DLis1* locus shows significant transcriptional complexity. We have identified two different 5′ exons in *DLis1* suggesting the presence of two separate promoters. Although the transcripts derived from the two 5′ exons have identical coding regions, they are differentially represented in stage-specific cDNA libraries, suggesting that the choice of promoters could be developmentally regulated. The observation that the $DLis1^{11702}$ insertion is a hypomorphic allele, despite its location in an exon, raises the possibility that the transposon insertion does not affect transcripts originating from the second downstream promoter (see Fig. 1C).

In contrast to the viable $DLis1^{11702}$ mutation, all nine EMS alleles and the P-insertion allele $DLis1^{13209}$ are late larval or early pupal lethals, suggesting that this represents the strong loss-of-function phenotype. These alleles appear to be largely similar in strength, based on the incidence of dorsal appendage defects encountered in eggs laid by heteroallelic females. In this context it is noteworthy that a deficiency for the region, *Df(2R)JP8*, has a milder dorsal appendage phenotype compared to the lethal alleles we have identified (see Table 1; data not shown). One possibility is that the deficiency represents the null phenotype and that the *DLis1* alleles encode gain-of-function or antimorphic mutations. This appears unlikely since all nine EMS alleles, as well as the $DLis1^{13209}$ allele which results from a P insertion in a noncoding region, have similar phenotypes. Another possibility is that *Df(2R)JP8* uncovers additional loci that partially suppress the effects of loss of *DLis1*. We

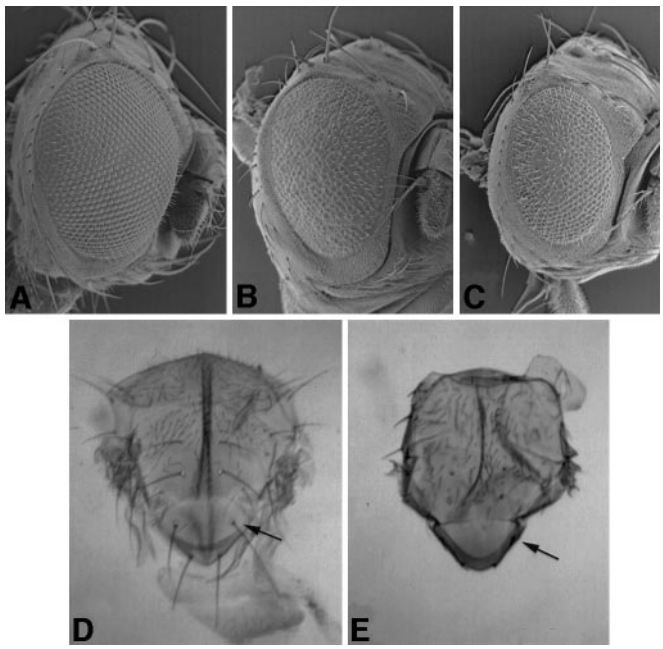

FIG. 7. *DLis1* alleles show genetic interactions with Gl^1 mutations. (A–C) Scanning electron micrographs of eyes from male flies at the same magnification. (A) Wild-type eyes are characterized by a regular array of ommatidia and mechanosensory bristles. (B) Eyes from Gl^1 flies are smaller and appear rough. The bristles are abnormally arranged. (C) Adult escapers of the genotype $DLis^{8.25.3}/DLis1^{11702}$; Gl^1/+ have eyes that are also rough and further reduced in size. (D) Scutellum from a wild-type fly, with arrow indicating a macrochetae. (E) In $DLis^{8.25.3}/DLis1^{11702}$; Gl^1/+ escapers, the scutellar bristles are frequently absent or highly reduced. Bristles in the notum are also affected.

favor this alternative since this deficiency also removes the *kinesin heavy chain* gene that encodes a plus-end-directed microtubule motor involved in cytoskeletal motility (Saxton *et al.*, 1991; Y. Lei and R. Warrior, unpublished data).

The sequence analysis of *DLis1* mutant alleles highlights the importance of the C-terminal residues in the protein. Interestingly, the phenotype of the $DLis1^{11.4.3}$ allele that deletes only the last 16 residues is as strong as that of $DLis1^{3.1.2}$, which lacks the majority of the protein (see Fig. 1A and Table 1). Similarly in human LIS1, a deletion of the last 23 residues results in a moderately severe form of lissencephaly (Pilz *et al.*, 1998). These data indicate that the seventh GH-WD repeat is very critical for the function or the stability of this class of proteins. As mentioned earlier, Lis1 proteins are predicted to fold into a seven-bladed β-propeller structure similar to the GH-WD domain protein β-transducin. In β-transducin, residues from the first and the seventh WD repeats overlap to form a "Velcro snap" that holds the propeller structure together (reviewed in Smith *et al.*, 1999). It is likely that the loss of the C-terminal residues in $DLis1^{11.4.3}$ and the mutant human protein affects the integrity of this structure. Thus even slightly truncated forms of the protein may not form an appropriate tertiary structure.

Potential Cellular Roles for DLis1

Homozygosity for strong mutations in *DLis1* results in larval lethality, demonstrating that it is an essential gene. In this study we have taken advantage of viable transheterozygous combinations of *DLis1* alleles that result in partial loss of function, to demonstrate the involvement of *DLis1* in nuclear migration during oogenesis. Mutations in *DLis1* disrupt the localization of *grk* mRNA and protein and result in partial ventralization of the eggshell. The distribution of *bcd* and *osk* transcripts is unaffected in *DLis1* mutants, making it unlikely that there is a general requirement for DLis1 activity in RNA localization. We find that the mislocalization of *grk* message is correlated with incorrect positioning of the oocyte nucleus. Based on our phenotypic analysis, we infer that the primary defect lies in nuclear migration (Fig. 5). However, an alternative explanation could be that the nuclei fail to be anchored to the oocyte cortex and thus are improperly localized. Other developmental processes that involve nuclear migration include formation of the syncytial blastoderm during early embryogenesis and morphogenesis of the eye imaginal disc. We have preliminary evidence that *DLis1* affects migration of nuclei during imaginal disc development since *DLis1* mutant flies that have been rescued to adulthood using an Hsp70 → DLis1 transgene have rough eyes (J. Duncan and R. Warrior, unpublished data).

There are several lines of evidence to suggest that Lis1 proteins may affect nuclear migration by modulating dynein motor function. In *Aspergillus,* mutations in the cytoplasmic dynein heavy chain (*nudA*) and light chain (*nudG*) genes result in nuclear migration defects similar to those in *nudF* mutants, suggesting that all three genes act in a common pathway. A screen for suppressers of *nudF* recovered compensatory mutations in *nudA,* indicating that *nudF* acts upstream of dynein (Xiang *et al.*, 1995b; Willins *et al.*, 1997). Consistent with this, in yeast, mutations in the dynein heavy chain and the *DLis1* homolog *pac1* have similar phenotypes (Geiser *et al.*, 1997). Our finding that a reduction in *DLis1* activity affects dynein localization to the posterior of the oocyte lends further support to this idea. In addition, we observe strong genetic interactions between *DLis1, Gl,* and *Dhc64C,* suggesting that these genes are functionally linked. Similar results have been reported in a recent study by Swan *et al.* (1999). Using a stronger allelic combination, these authors observe relatively more severe defects and find that *DLis1* affects dynein localization as early as stage 1.

Given the involvement of cytoplasmic dynein in a range of cellular processes, one might expect mutations in *DLis1* to affect other developmental events that are linked mechanistically. Specific combinations of *Dhc64C* alleles that result in female sterility reveal a requirement for dynein in the synchronized divisions that give rise to the 16-cell cyst from which the oocyte differentiates, as well as in oocyte specification (McGrail and Hays, 1997). We have observed that germ-line clones lacking *DLis1* function arrest early in oogenesis and result in egg chambers containing reduced numbers of germ-line cells (Y. Lei and R. Warrior, unpublished data). Liu *et al.* (1999) have recently shown that this results from a requirement for *DLis1* activity in germ-line cell division and maintenance of fusome integrity. Furthermore, determination of oocyte identity is also dependent on interactions between *DLis1* and *Bicaudal-D, egalitarian,* and *Dhc64C* (Swan *et al.*, 1999). These studies underscore the pleiotropic requirement for *DLis1* at multiple stages of oocyte development. Vertebrate *Lis1* genes are also likely to have multiple functions since *Lis1* null mouse embryos suffer early postimplantation lethality (Hirotsune *et al.*, 1998).

While *DLis1* and its fungal homologs affect nuclear migration, Lis1 proteins in mice and humans affect neuronal migration. Recent studies in *Drosophila* indicating that disruptions in cytoskeletal motors perturb both nuclear and neuronal migration could provide a way to reconcile these seemingly distinct phenomena. Mutations in *Drosophila dynein light chain, Gl,* and *Dhc64C* cause defects in axonal pathfinding and synaptogenesis during pupal stages (Phillis *et al.*, 1996; Murphey *et al.*, 1999). We are currently examining *DLis1* mutants to see if axonal pathfinding is perturbed.

In addition to its interaction with dynein, it is possible that DLis1 can affect microtubules or other cytoskeletal components. Mutations in genes such as *maelstrom, cappuccino,* and *spire* that affect microtubule function are also known to disrupt mRNA localization during oogenesis (Manseau and Schupbach, 1989; Emmons *et al.*, 1995; Clegg *et al.*, 1997). Human LIS1 has been shown to copurify with microtubules and can reduce the rate of microtubule catas-

trophe *in vitro* (Sapir *et al.*, 1997). Thus loss of LIS1 activity would be predicted to increase the catastrophe rate and result in a shortening of the average microtubule length. If mutations in *DLis1* decrease microtubule stability, this could provide an explanation for the nuclear migration defects observed in mutants. The fact that we did not observe a generalized mislocalization of mRNAs and *Kin:βgal* in *DLis1* mutant oocytes argues against this hypothesis. However, our analysis was based on animals with reduced *DLis1* activity rather than in a complete loss-of-function background, and it is possible that nuclear migration is more sensitive to subtle destabilization of the microtubule network.

Another intriguing aspect of *Lis1* activity in mammals is that it has been found to copurify with platelet-activating factor acetylhydrolase, PAF-AH(Ib), an enzyme that inactivates a lipid signal, platelet-activating factor (PAF; Hattori *et al.*, 1994). The enzyme consists of a heterotrimeric complex of Lis1 and two related subunits, both of which have catalytic activity (Hattori *et al.*, 1994, 1995). While the biological role of PAF-AH(Ib) is unclear, neuronal migration *in vitro* is sensitive to PAF and PAF analogs, suggesting that this association may have some functional significance (Adachi *et al.*, 1997; McNeil *et al.*, 1999). Although a *Drosophila* homolog of the mammalian PAF-AH catalytic subunits can be found in the sequence database, the predicted protein is unlikely to be enzymatically active since it contains an amino acid substitution that replaces an essential residue in the catalytic site (C. Hogan and R. Warrior, unpublished data).

ACKNOWLEDGMENTS

We thank C. Berg for generously providing stocks, reagents, and insightful advice. We also thank R. Lehman, D. McKearin, E. Holzbaur, T. Schupbach, and T. Hays for sharing *Drosophila* stocks and antibodies. Finally we gratefully acknowledge the important material and intellectual contributions made by K. Arora over the period of this study. This research was supported by Grant GM48659 from the NIH and by funds from the March of Dimes Birth Defects Foundation. The Bio-Rad MRC 600 confocal microscope used in this was work was partially funded through NSF Multiuser Grant BIR 9419941.

REFERENCES

Adachi, T., Aoki, J., Manya, H., Asou, H., Arai, H., and Inoue, K. (1997). PAF analogues capable of inhibiting PAF acetylhydrolase activity suppress migration of isolated rat cerebellar granule cells. *Neurosci. Lett.* **235,** 133–136.

Beckwith, S. M., Roghi, C. H., and Morris, N. R. (1995). The genetics of nuclear migration in fungi. *In* "Genetic Engineering, Principles and Methods," Vol. 17, pp. 165–180. Plenum, New York.

Berleth, T., Burri, M., Thoma, G., Bopp, D., Richstein, S., Frigerio, G., Noll, M., and Nusslein-Volhard, C. (1988). The role of localization of *bicoid* RNA in organizing the anterior pattern of the Drosophila embryo. *EMBO J.* **7,** 1749–1756.

Clark, I., Giniger, E., Ruohola-Baker, H., Jan, L. Y., and Jan, Y. N. (1994). Transient posterior localization of a kinesin fusion protein reflects anteroposterior polarity of the *Drosophila* oocyte. *Curr. Biol.* **4,** 289–300.

Clegg, N. J., Frost, D. M., Larkin, M. K., Subrahmanyan, L., Bryant, Z., and Ruohola-Baker, H. (1997). *maelstrom* is required for an early step in the establishment of Drosophila oocyte polarity: Posterior localization of *grk* mRNA. *Development* **124,** 4661–4671.

Cunniff, J., Chiu, Y.-H., Morris, N. R., and Warrior, R. (1997). Characterization of *DnudC*, the Drosophila homolog of an Aspergillus gene that functions in nuclear motility. *Mech. Dev.* **66,** 55–68.

Emmons, S., Phan, H., Calley, J., Chen, W., James, B., and Manseau, L. (1995). *cappuccino*, a *Drosophila* maternal effect gene required for polarity of the egg and embryo, is related to the vertebrate *limb deformity* locus. *Genes Dev.* **9,** 2482–2494.

Ephrussi, A., Dickinson, L. K., and Lehmann, R. (1991). *oskar* organizes the germ plasm and directs localization of the posterior determinant *nanos*. *Cell* **66,** 37–50.

Fan, S., and Ready, D. (1997). *Glued* participates in distinct microtubule-based activities in Drosophila eye development. *Development* **124,** 1497–1507.

Fischer-Vize, J. A., and Mosley, K. L. (1994). *marbles* mutants: Uncoupling cell determination and nuclear migration in the developing *Drosophila* eye. *Development* **120,** 2609–2618.

Foe, V. E., Odell, G. M., and Edgar, B. M. (1993). Mitosis and morphogenesis in the *Drosophila* embryo: Point and counterpoint. *In* "The Development of *Drosophila melanogaster*," pp. 149–300. Cold Spring Harbor Laboratory Press, Cold Spring Harbor, NY.

Garcia-Higuera, I., Fenoglio, J., Li, Y., Lewis, C., Panchenko, M. P., Reiner, O., Smith, N. F., and Neer, E. J. (1996). Folding of proteins with WD-repeats: Comparison of six members of the WD-repeat superfamily to the G protein beta subunit. *Biochemistry* **35,** 13985–13944.

Geiser, J., Schott, E., Kingsbury, T., Cole, N., Totis, L., Bhattacharyya, G., He, L., and Hoyt, M. (1997). *Saccharomyces cerevisiae* genes required in the absence of the CIN8-encoded spindle motor act in functionally diverse mitotic pathways. *Mol. Biol. Cell.* **8,** 1059–1524.

Gill, S. R., Schroer, T. A., Szilak, I., Steuer, E. R., Sheetz, M. P., and Cleveland, D. W. (1991). Dynactin, a conserved, ubiquitously expressed component of an activator of vesicle motility mediated by cytoplasmic dynein. *J. Cell Biol.* **115,** 1639–1650.

Giniger, E., Wells, W., Jan, L. Y., and Jan, Y. N. (1993). Tracing neurons with a kinesin-betagalactosidase fusion protein. *Roux's Arch. Dev. Biol.* **202,** 112–122.

Gonzalez-Reyes, A., Elliott, H., and St Johnston, D. (1995). Polarization of both major body axes in Drosophila by gurken–torpedo signalling. *Nature* **375,** 654–658.

Harte, P., and Kankel, D. (1982). Genetic analysis of mutations at the *Glued* locus and interacting loci in *Drosophila melanogaster*. *Genetics* **101,** 477–501.

Hattori, M., Adachi, H., Tsujimoto, M., Arai, H., and Inoue, K. (1994). Miller–Dieker lissencephaly gene encodes a subunit of brain platelet-activating factor. *Nature* **370,** 216–218.

Hattori, M., Adachi, H., Tsujimoto, M., Arai, H., and Inoue, K. (1995). Cloning and expression of a cDNA encoding the beta-subunit (30 kDa subunit) of bovine platelet factor acetylhydrolase. *J. Biol. Chem.* **270,** 31345–31352.

Hays, T. S., Porter, M. E., McGrail, M., Grissom, P., and Gosch, P. (1994). A cytoplasmic dynein motor in *Drosophila:* Identification and localization during embryogenesis. *J. Cell. Sci.* **107,** 1557–1569.

Hirokawa, N. (1998). Kinesin and dynein superfamily proteins and the mechanism of organelle transport. *Science* **279,** 519–526.

Hirotsune, S., Fleck, M. W., Gambello, M. J., Bix, G. J., Chen, A., Clark, G. D., Ledbetter, D. H., McBain, C. J., and Wynshaw-Boris, A. (1998). Graded reduction in *Pafah1b1* (*Lis1*) activity results in neuronal migration defects and early embryonic lethality. *Nat. Genet.* **19,** 333–339.

Holzbaur, E., and Vallee, R. B. (1994). Dyneins: Molecular structure and cellular function. *Annu. Rev. Cell. Biol.* **10,** 339–372.

Holzbaur, E. L. F., Hammarback, J. A., Paschal, B. M., Kravit, N. G., Pfister, K. K., and Vallee, R. B. (1991). Homology of a 150K cytoplasmic dynein-associated polypeptide with the *Drosophila* gene *Glued*. *Nature* **351,** 579–583.

Kim Ha, J., Smith, J. L., and Macdonald, P. M. (1991). *oskar* mRNA is localized to the posterior pole of the Drosophila oocyte. *Cell* **66,** 23–35.

Li, M.-G., McGrail, M., Serr, M., and Hays, T. (1994). Drosophila cytoplasmic dynein, a microtubule motor that is asymmetrically localized to the oocyte. *J. Cell. Biol.* **126,** 1475–1494.

Liu, Z., Xie, T., and Steward, R. (1999). *Lis1,* the Drosophila homolog of a human lissencephaly disease gene, is required for germline cell division and oocyte differentiation. *Development* **126,** 4477–4488.

Lo Nigro, C., Chong, C. S., Smith, A. C., Dobyns, W. B., Carrozzo, R., and Ledbetter, D. H. (1997). Point mutations and an intragenic deletion in *LIS1,* the lissencephaly causative gene in isolated lissencephaly sequence and Miller–Dieker syndrome. *Hum. Mol. Genet.* **6,** 157–164.

Lupas, A. (1996). Prediction and analysis of coiled-coil structures. *Methods Enzymol.* **266,** 513–525.

Manseau, L., and Schupbach, T. (1989). *cappuccino* and *spire:* Two unique maternal-effect loci required for both anteroposterior and dorsoventral patterns of the *Drosophila* embryo. *Genes Dev.* **3,** 1437–1452.

McGrail, M., Gepner, J., Silvanovich, A., Ludman, S., Serr, M., and Hays, T. S. (1995). Regulation of cytoplasmic dynein function in vivo by the *Drosophila* Glued complex. *J. Cell. Biol.* **131,** 411–425.

McGrail, M., and Hays, T. (1997). The microtubule motor cytoplasmic dynein is required for spindle orientation during germline cell divisions and oocyte differentiation in Drosophila. *Development* **124,** 2409–2419.

McNeil, R. S., Swann, J. W., Brinkley, B. R., and Clark, G. D. (1999). Neuronal cytoskeletal alterations evoked by a platelet-activating factor (PAF) analogue. *Cell Motil. Cytoskeleton*. **43,** 99–113.

Miller, B. A., Zhang, M. Y., Gocke, C. D., De Souza, C., Osmani, A. H., Lynch, C., Davies, J., Bell, L., and Osmani, S. A. (1999). A homolog of the fungal nuclear migration gene *nudC* is involved in normal and malignant human hematopoiesis. *Exp. Hematol.* **27,** 742–750.

Morris, S. M., Anaya, P., Xiang, X., Morris, N. R., May, G. S., and Yu-Lee, L.-Y. (1997). A prolactin-inducible T cell gene product is structurally similar to the *Aspergillus nidulans* nuclear movement protein NUDC. *Mol. Endocrinol.* **7,** 229–236.

Murphey, R. K., Caruccio, P. C., Getzinger, M., Westgate, P. J., and Phillis, R. W. (1999). Dynein–dynactin function and sensory axon growth during Drosophila metamorphosis: A role for retrograde motors. *Dev. Biol.* **209,** 86–97.

Neuman-Silberberg, F. S., and Schupbach, T. (1993). The Drosophila dorsoventral patterning gene *gurken* produces a dorsally localized RNA and encodes a TGF alpha-like protein. *Cell* **75,** 165–174.

Neuman-Silberberg, F. S., and Schupbach, T. (1996). The Drosophila TGF-alpha-like protein Gurken: Expression and cellular localization during Drosophila oogenesis. *Mech. Dev.* **59,** 105–113.

Nilson, L. A., and Schupbach, T. (1999). EGF receptor signaling in Drosophila oogenesis. *Curr. Top. Dev. Biol.* **44,** 203–243.

Osmani, A. H., Osmani, S. A., and Morris, N. R. (1990). The molecular cloning and identification of a gene product specifically required for nuclear movement in *Aspergillus nidulans. J. Cell. Biol.* **111,** 543–541.

Peterfy, M., Gyuris, T., Basu, R., and Takacs, L. (1994). Lissencephaly-1 is one of the most conserved proteins between mouse and human: A single amino-acid difference in 410 residues. *Gene* **150,** 415–416.

Peterfy, M., Gyuris, T., Grosshans, D., Cuaresma, C. C., and Takacs, L. (1998). Cloning and characterization of cDNAs and the gene encoding the mouse platelet-activating factor acetyl hydrolase Ib subunit/lissencephaly-1 protein. *Genomics* **47,** 200–206.

Phillis, R., Statton, D., Caruccio, P., and Murphey, R. K. (1996). Mutations in the 8 kDa dynein light chain gene disrupt sensory axon projections in the Drosophila imaginal CNS. *Development* **122,** 2955–2963.

Pilz, D. T., Matsumoto, N., Minnerath, S., Mills, P., Gleeson, J. G., Allen, K. M., Walsh, C. A., Barkovich, A. J., Dobyns, W. B., Ledbetter, D. H., and Ross, M. E. (1998). LIS1 and XLIS (DCX) mutations cause most classical lissencephaly, but different patterns of malformation. *Hum. Mol. Genet.* **7,** 2029–2037.

Reiner, O., Carrozzo, R., Shen, Y., Wehnert, M., Faustinella, F., Dobyns, W. B., Caskey, C. T., and Ledbetter, D. H. (1993). Isolation of a Miller–Dieker lissencephaly gene containing G protein b-subunit-like repeats. *Nature* **364,** 717–721.

Reinsch, S., and Gonczy, P. (1998). Mechanisms of nuclear positioning. *J. Cell Sci.* **111,** 2283–2295.

Roth, S., Neuman-Silberberg, F. S., Barcelo, G., and Schupbach, T. (1995). *cornichon* and the EGF receptor signaling process are necessary for both anterior–posterior and dorsal–ventral pattern formation in Drosophila. *Cell* **81,** 967–978.

Sapir, T., Elbaum, M., and Reiner, O. (1997). Reduction of microtubule catastrophe events by LIS1, platelet-activating factor acetylhydrolase subunit. *EMBO J.* **16,** 6977–6984.

Sauer, F. C. (1935). Mitosis in the neural tube. *J. Comp. Neurol.* **62,** 377–405.

Saxton, W. M., Hicks, J., Goldstein, L. S. B., and Raff, E. C. (1991). Kinesin heavy chain is essential for viability and neuromuscular functions in Drosophila, but mutants show no defects in mitosis. *Cell* **64,** 1093–1102.

Schatten, G. (1982). Motility during fertilization. *Int. Rev. Cytol.* **79,** 59–163.

Schupbach, T., and Wieschaus, E. (1991). Female sterile mutations on the second chromosome of *Drosophila melanogaster.* II. Mutations blocking oogenesis or altering morphology. *Genetics* **129,** 1119–1136.

Smith, T., Gaitatzes, C., Saxena, K., and Neer, E. (1999). The WD repeat: A common architecture for diverse functions. *Trends Biochem. Sci.* **24,** 181–185.

Sondek, J., Bohm, A., Lambright, D. G., Hamm, H. E., and Sigler, P. B. (1996). Crystal structure of a G-protein beta gamma dimer at 2.1A resolution. *Nature* **379,** 369–374.

Swan, A., Nguyen, T., and Suter, B. (1999). *Drosophila Lissencephaly-1* functions with *Bic-D* and dynein in oocyte determination and nuclear positioning. *Nat. Cell Biol.* **1,** 444–449.

Swaroop, A., Swaroop, M., and Garen, A. (1987). Sequence analysis of the complete cDNA and encoded polypeptide for the *Glued* gene of *Drosophila melanogaster*. *Proc. Natl. Acad. Sci. USA* **84,** 6501–6505.

Tomlinson, A. (1985). The cellular dynamics of pattern formation in the eye of Drosophila. *J. Embryol. Exp. Morphol.* **89,** 313–331.

Verheyen, E., and Cooley, L. (1994). Looking at oogenesis. *Methods Cell Biol.* **44,** 545–561.

Willins, D., Liu, B., Xiang, X., and Morris, N. (1997). Mutations in the heavy chain of cytoplasmic dynein suppress the nudF nuclear migration mutation of *Aspergillus nidulans*. *Mol. Gen. Genet.* **255,** 194–200.

Xiang, X., Osmani, A., Osmani, S., Xin, M., and Morris, N. R. (1995a). *NudF,* a nuclear migration gene in *Aspergillus nidulans,* is similar to the human *LIS-1* gene required for neuronal migration. *Mol. Biol. Cell.* **6,** 297–310.

Xiang, X., Roghi, C., and Morris, N. R. (1995b). Characterization and localization of the cytoplasmic dynein heavy chain in *Aspergillus nidulans*. *Proc. Natl. Acad. Sci. USA* **92,** 9890–9894.

Yang, J., Saxton, W., and Goldstein, L. (1988). Isolation and characterization of the gene encoding the heavy chain of Drosophila kinesin. *Proc. Natl. Acad. Sci. USA* **85,** 1864–1868.

Received for publication March 16, 2000
Revised June 28, 2000
Accepted June 28, 2000